Heat transfer performance of structured catalytic reactors packed with metal foam supports: Influence of wall coupling

S. Razza [a,b], T. Heidig [a], E. Bianchi [a,b], G. Groppi [b], W. Schwieger [a], E. Tronconi [b], H. Freund [a,*]

[a] Lehrstuhl für Chemische Reaktionstechnik, Friedrich-Alexander-Universität Erlangen-Nürnberg, Egerlandstr. 3, Erlangen D-91058, Germany
[b] Laboratory of Catalysis and Catalytic Processes, Dipartimento di Energia, Politecnico di Milano, via Lambruschini 4, Milano 20156, Italy

Based on previous lab-scale heat transfer experiments performed in a test tube filled with metallic foams, extensive simulations of conjugated heat transfer were performed to systematically investigate the role of different coupling scenarios between the foam structure and the tube wall, using a 3D scanned foam geometry to enable the comparison of simulation results with experiments. The goal of this analysis is to gain insight into the prominent role of the wall coupling for radial heat transfer in a structured catalytic reactor packed with metal foams as catalyst supports. In the current numerical investigation the focus is on the characterization of the contact area between the foam and the reactor wall. Starting from perfect contact between the two, the contact area was decreased by selecting randomly some boundary spots of the foam and considering them as adiabatic. Moreover, the local distribution of the adiabatic struts was restricted to regions near the reactor inlet to additionally investigate the influence of the local distribution of the adiabatic struts at same overall contact areas. Eventually, all the contacts between the foam and the reactor wall were considered adiabatic as the other limiting case, wherein heat transfer at the foam/wall interface was governed solely by convection. The numerical analysis revealed that even if only a limited fraction of the struts have a direct contact with the tube wall, the heat transfer rate is significantly enhanced in comparison to the adiabatic case. In analogy with the previous experimental study, the numerical investigation was carried out for two different gases, nitrogen and helium, in order to address the influence of the thermal conductivity of the fluid phase. For further experimental verification, additional heat transfer measurements were performed for the case of a foam directly sintered to the tube in order to realize a perfect contact between foam and wall.

Keywords: Metal foam, Heat transfer, Process intensification, Structured reactors

1. Introduction

This work presents a numerical examination of heat transfer in metallic open-cell foams in order to evaluate the potential regarding their use as catalyst supports in catalytic reactors. Open-cell foams, also called solid sponges, are irregular cellular structures made of various materials from metals to ceramics [1]. In our current work, the focus is on metal foams for industrial applications as catalyst carriers due to their superior heat conductivity. Solid open-cell foams are very interesting because they exhibit a unique combination of physical properties such as high rigidity, low specific weight, high specific surface area and high gas permeability [2–8]. Therefore, they are suitable for applications in the automotive industries, as light weight construction materials, silencers, flame arresters, heaters, and for electrochemical applications [9–12]. Their high thermal conductivity makes them also an interesting candidate as catalyst supports for both, exothermic and endothermic processes, wherein thermal control is critical [13]. Open-cell metal foams can minimize hot spots and reduce thermal shock, thereby improving selectivity and preventing catalyst deactivation. These promising characteristics suggest replacing conventional packed-bed catalyst pellets with catalytically functionalized (e.g. coated) metal foams. In fact, when using metal foams as catalyst supports, higher yield and selectivity can be achieved particularly in heat transfer limited processes due to the improved temperature control and heat management [14,15]. In conventional particle packed-bed reactors for strongly exothermic heterogeneously catalyzed reactions, a multitude of tubes of

Article history:
Received 4 December 2015
Received in revised form 19 February 2016
Accepted 21 February 2016
Available online 3 April 2016

* Corresponding author.
E-mail address: hannsjoerg.freund@fau.de (H. Freund).

Published Journal Article available at: http://dx.doi.org/10.1016/j.cattod.2016.02.058

Nomenclature

List of symbols

c_p	Specific heat capacity ($kJ\,(kg\,K)^{-1}$)
h	Enthalpy per unit mass ($kJ\,kg^{-1}$)
I	Identity matrix
k	Thermal conductivity ($W\,(m\,K)^{-1}$)
L	Reactor length (m)
P	Pressure (Pa)
ppi	Number of pores per inch
R	Gas constant ($kJ\,(mol\,K)^{-1}$)
T	Temperature (K)
T_i	Area weighted average temperature (K)
T^*	Inlet temperature (K)
$\vec{u}$	Fluid velocity ($m\,s^{-1}$)
z	Spatial position (m)

Greek symbols

ε	Porosity
ϑ	Non-dimensional temperature
ρ	Density ($kg\,m^{-3}$)
τ	Viscous stress tensor ($kg\,m^{-1}\,s^{-2}$)
μ	Dynamic viscosity ($kg\,(s\,m)^{-1}$)

Subscripts

f	Fluid phase
gas	Gas phase
H	Hydrodynamic
tube	At the tube wall
s	Solid
T	Total

relatively small diameter is placed in parallel. While the number of parallel tubes is determined by the required production rate, the diameter of the tubes is chosen as to match the required heat exchange area. This design, however, causes both, high investment costs for the multitubular reactor (several thousand welded tubes) as well as high operating costs due to significant pressure drop. To minimize the pressure drop, the catalyst pellets should be large. This, however, will decrease the catalyst effectiveness factor for full-bodied catalyst [14] and lead to a higher void fraction of the bed as well as to strong oscillations in both, radial porosity as well as radial velocity profiles [16]. All these issues that arise from the various different requirements can in principle be solved by employing metal foams as catalyst supports. As mentioned above, metallic foams are particularly suited for heat-transfer limited processes. In a recent study, it has been demonstrated that metal foams possess superior heat transfer performance due to the dominant contribution of heat conduction in the continuous solid phase [13,17]. The more efficient heat transfer would allow for the use of tubes of larger diameter, thereby reducing the number of required tubes. In addition, the higher porosity of the foams also significantly reduces the pressure drop.

A variety of industrial processes of potential interest can be mentioned, e.g. highly endothermic reactions such as, e.g., dehydrogenation reactions (i.e. cyclohexane to benzene or ethyl benzene to styrene) and steam reforming of methane for syngas production [18]. Even more examples can be given for the class of strongly exothermic reactions, e.g. partial oxidation of hydrocarbons [19], where the desired product is an intermediate and short contact time is required [20,21], alkylation reactions (e.g. benzene to ethyl benzene), oxychlorination (e.g. acetic acid to vinyl acetate), and hydrogenation reactions, such as Fischer-Tropsch synthesis [14] and methanol synthesis [22]. All these processes can profit from the enhanced heat transport in the foam support structures.

Originally, foams were designed for applications in energy absorption, filtration and noise reduction, and not necessarily endowed with optimal structural characteristics for catalytic applications. As a result, high manufacturing costs make them today still less competitive with more common supports in terms of both, fabrication material and geometry as well as catalyst hold-up [2,9,23]. Therefore, it is the current task to make the design, fabrication and catalytic application of metal foams as competitive as possible with the state-of-the-art pellets. For this, it is at first essential to gain a deep understanding of the underlying principles and of the geometry-transport interactions. In this regard, one aspect is the investigation of the heat transfer performance of a novel reactor design using metal foams as catalyst support, and in particular the investigation of the influence of the wall coupling in order to derive guidelines for proper design.

In our previous work on heat transfer in metal foams [13,24,25], we focused on the experimental investigation of conjugated heat transfer between the gas phase and the metal foam and compared the experimental results with numerical simulations. Moreover, we analyzed the influence of the gap between metal foam and reactor wall and provided correlations for different scenarios [25]. These studies pointed out the resistance at the boundary between foam and tube as a major effect to be considered in the evaluation of the overall heat transfer performance.

The present numerical investigation was inspired by the question for proper design and fitting of metal foams as a catalyst support for gas phase reactions in industrial applications, where the coupling between the foam and the reactor tube will be not perfect due to the imperfect matching of the two or the possible damage during loading and replacement operations. The question, however, is whether a complete perfect fitting is necessary at all, or whether it is sufficient to realize the perfect contact only for a certain fraction of the struts at the tube wall. Of course, the design questions then are: what is the required fraction of perfect strut contact, and where in the reactor should these strut contacts are positioned?

To answer these questions, the coupling between the reactor tube and the open-cell metal foam loaded as a catalyst support was simulated in detail, varying the location and the number of connections between the two. As model geometry, a 3D scan of the geometry of a metal foam sample from our previous experimental analysis was considered to enable the comparison of simulation results with experiments.

2. Materials and methods

The particularity of the metal foam materials is their structure with high specific surface area and high porosity of typically 75–95%. Those characteristics offer excellent potential for high performance in terms of low resistance to fluid flow, high gas-solid mass and heat transfer, and, particularly for foams made of conductive metals, high radial and axial heat transfer efficiency. Furthermore, in comparison to honeycomb monoliths, metal foams allow for radial mixing thanks to the interconnected continuous pore space and the flow turbulence produced by their irregular spongy structure [2].

The case study presented in this work concerns the thermal analysis of a cold gas passing through an externally heated tube filled with an open-cell metal foam. Two gases with different thermal conductivity are investigated, namely N_2 and He. The feed passes through the tube packed with a metal foam made of Al alloy (6101-T6) and is thereby heated up by the tube.

2.1. Foam material

The Al alloy foam used in both previous experiments and simulations is not composed of pure aluminum (~98%), but is enriched with other elements such as Si and Mg, and artificially aged in order to enhance the properties of the original material. Starting from a 20 ppi nominal panel, the foam sample is obtained by electro erosion. This technique permits a precise cut without damaging the structure of the sample [26].

The open void fraction in a cellular solid is defined as the ratio between the accessible void volume and the total volume. From gravimetric analysis and from previous considerations [2,11,13,14], it is possible to identify two different porosities: the total porosity ε_T, which includes all kinds of void space, and the hydrodynamic porosity ε_H which only considers the macroscopic accessible void space. The hydrodynamic porosity is the relevant parameter for investigations regarding mass transfer and pressure drop of foams used as catalyst supports [27,28] as well as when heat transfer contributions by dispersive and radiative mechanisms [29] are considered. On the other hand, the total porosity is relevant to assess the conductive contribution to heat transfer. For the foam herein investigated the same value $\varepsilon_T = \varepsilon_H = 89.7\%$ was obtained [13], thus no inaccessible void space was identified.

Concerning the thermophysical properties, the density of the metal foam is 2.70 g/cm^3 [29] and the heat capacity is 903 J/(kg K) measured at room temperature. The thermal conductivity of the Al alloy is assumed to be constant in the investigated temperature range at a value of 218 W/(m K). From previous work [13] the contribution of radiation to the overall heat transfer for such highly conductive foams at the considered temperatures is known to be insignificant, therefore, the influence of radiation is neglected in this study.

The geometry of the investigated foam sample is a cylinder of 50 mm in length and 28 mm in diameter. Three axial holes of 3.28 mm diameter were drilled in the sample at three radial positions, centerline, 7 mm, and 9 mm from the center (Fig. 1). These holes allowed for the insertion of three sliding thermocouples for the measurement of internal temperature profiles.

2.2. Gas properties

Two different gases, namely nitrogen and helium, were considered as representative of low conductive gases such as, e.g., air, and high conductive gases such as, e.g., syngas (CO/H_2), respectively. The thermodynamic and transport properties of the fluid phase are assumed to be constant and calculated based on the average temperature of the simulated run for either N_2 or He, and compiled in Table 1. The properties for nitrogen are calculated at 629 K and for helium at 679 K.

2.3. Experimental setup

Simulation results are compared with the experimental ones, collected in a setup described in detail elsewhere [13,24]. Two configurations were adopted. In the first case, the heated tube is filled with a loose cylinder of an Al foam of 5 cm in length. In the second setup, in contrast, the foam is sintered directly into the heating tube made of aluminum by heating at 550–600 °C, so as to ensure continuity between the foam struts and the reactor wall by diffusion bonding between the tube wall and the tip of the foam struts.

The temperature profiles were collected by sliding the thermocouples from −5 mm to +50 mm with the origin of the axial coordinate at the beginning of the foam bed. The temperature was measured at different radial positions with the three thermocouples at the center, 7 mm, and 9 mm from the center for the loose foam, and two for the sintered foam with one at the center and the other at 9 mm from the centerline.

3. Simulation details

The mesh generator and the solver for the finite volume analysis were implemented in the open source environment OpenFOAM v2.1.1 [30], a general library of C++ classes for the numerical simulation of partial differential equations mainly used for computational fluid dynamics (CFD) simulations.

3.1. Mesh domain

The 3D mesh was generated on the basis of an X-ray microcomputed tomography scan [31,32] of the foam cylinder utilized in the experimental setup, with a resolution of 50 μm (see [13]). Both, gas and solid phase were meshed, and the grid refinement was checked until the simulation results converged to a stable solution. The necessary resolution thereby mainly depends on the mesh in the thinner struts of the foam. The final mesh consists of about 5.6 million elements, 90% of which are hexahedral.

The simulated subdomain is one fourth of the experimental tubular reactor of 28 mm diameter containing a foam bed of 50 mm length (Fig. 1). The selection of one fourth for the simulation runs has been chosen such that the holes for the thermocouples were excluded, in order to obtain as a result a uniform temperature profile, excluding the local variation of the flow due to the holes. Therefore, the selected subdomain contains only the unavoidable one quarter of the central hole (Fig. 1b). Details of the mesh grid can be seen in Fig. 3b.

3.2. Equations and solving conditions

The OpenFOAM model implemented in this work is able to couple the thermal flow in the fluid phase with the heat conduction in the solid phase. For the latter, the heat conduction equation is solved, while mass, momentum and energy conservation equations are solved for the fluid phase. The steady-state laminar Navier-Stokes equations are used since the flow considered in this study is laminar between Forchheimer and post-Forchheimer flow regime, with the Reynolds number lower than 300, calculated based on the cell diameter as characteristic length as obtained from tomography. In addition, the fluid is considered as an ideal gas, thus the equation of state $P = \rho RT$ is valid.

For the fluid phase, the mass conservation equation is given by:

$$\nabla\left(\rho\vec{u}\right) = 0$$

with ρ as the fluid density and u as the fluid velocity. Neglecting buoyancy effects, the conservation of momentum is:

$$\nabla\left(\rho\vec{u}\vec{u}\right) = -\nabla P + \nabla\tau$$

where P is the pressure and τ the viscous stress tensor. For a Newtonian fluid the viscous stress tensor is defined as:

$$\tau = \mu\left[\left(\nabla\vec{u}\right) + \left(\nabla\vec{u}\right)^T\right] - 2/3\mu\left[\left(\nabla\vec{u}\right)\vec{I}\right]$$

where μ is the dynamic viscosity of the fluid. The low viscosity of the simulated gases permits to neglect internal heat generation, gravitational potential energy and viscous forces, so the steady-state energy conservation equation can be written in enthalpy form:

$$\nabla\left(\rho h + 1/2\rho|u|^2\right)\vec{u} = \nabla\left(k_f/c_p\nabla h\right)$$

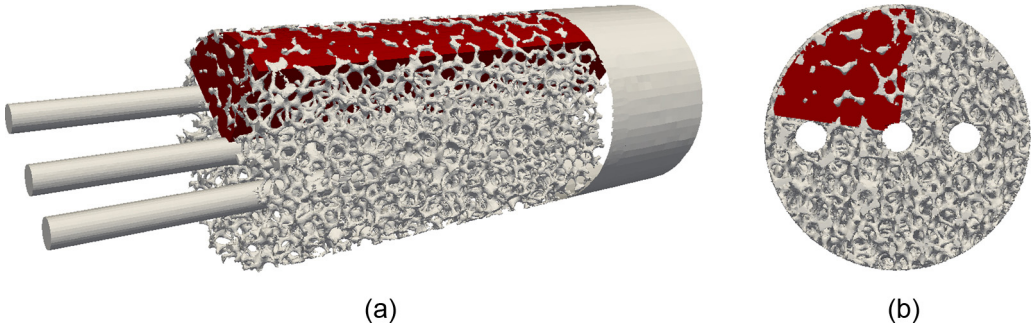

Fig. 1. Mesh domain for the solid phase, highlighting the selected quarter and the inlet region, axial view (a) and frontal view (b) with the holes for the three thermocouples.

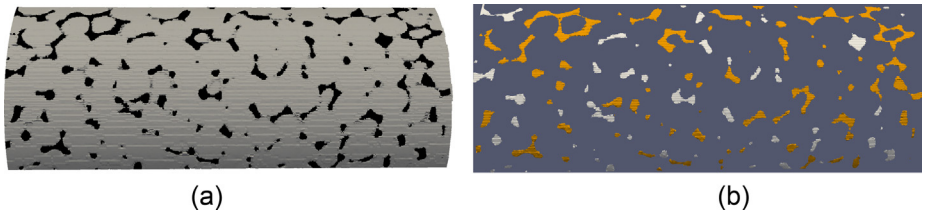

Fig. 2. View of the metal foam struts in contact with the reactor wall: the tube wall is colored in grey, and the end parts of the foam connected to the wall are shown in black (a). The connected spots are extracted as independent regions and labelled with a randomization algorithm as either being in contact (colored in white) or as adiabatic (orange). Figure (b) shows exemplarily a fraction of 30% connected strut area with the wall. (For interpretation of the references to color in this figure legend, the reader is referred to the web version of this article.)

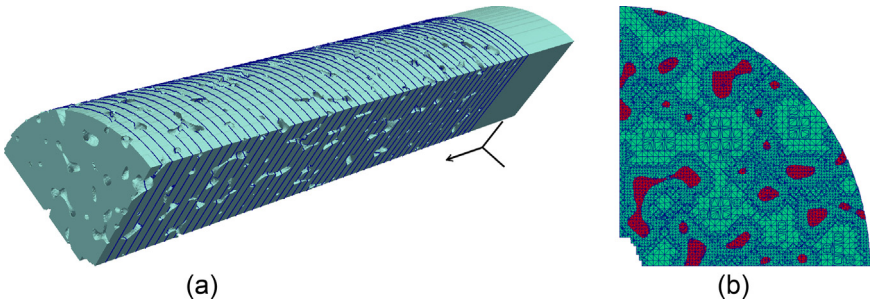

Fig. 3. Position of fifty slices used for the calculation of the area averaged gas temperature profile (a). Details of the mesh grid for one slice (b).

where k_f is the thermal conductivity of the fluid, c_p the specific heat capacity at constant pressure and h the enthalpy per unit mass.

The energy equation for the solid phase, without heat generation, is:

$$\nabla (k_S \nabla T) = 0$$

where k_S is the thermal conductivity of the solid and T the temperature.

Since the simulation results shall be compared with experimental data, the simulation boundary conditions are fixed in order to reproduce in a realistic way the experimental configuration. As described in a previous paper [13], a 30 Nl/min flow rate of gas, N_2 or He, is heated up from the nominal inlet temperature of 500 K. Thermodynamic properties are assumed constant for both solid and gas phase, calculated at the average temperature of the simulated run for either N_2 or He in the case of perfect contact between foam and reactor wall. From this previous study [13] it can also be concluded that the contribution of radiation to the overall heat transfer for the considered Al alloy foam at the given temperature range can be neglected.

As described above (Fig. 1), only one fourth of the whole cylindrical tube is reconstructed. Symmetric boundary conditions are applied for the state variables at the cut faces parallel to the tube axis. In this work, each end of the foam branches in contact with the tube wall was extracted as an independent region (Fig. 2). With a randomization algorithm that selects a fraction of the whole contact area, some strut/wall connections were set to adiabatic in order to impose the absence of conduction on that part of the foam (Fig. 2b).

The tube wall temperature boundary condition was adopted from measurements with the experimental setup and could be described by a 3rd order polynomial in dependence of the axial coordinate (Fig. 5).

At the solid-fluid boundary a no-slip condition is set for the velocity field. A zero gradient condition for the pressure field is

Table 1
Thermophysical properties used in the simulation of the two gases.

	Reference temperature [K]	Thermal conductivity [W/(m K)]	Molar weight [kg/kmol]	Specific heat [J/(kg K)]	Dynamic viscosity [Pa s]	Density [kg/m^3]
Nitrogen	629	0.046	28	1081	$2.99\ 10^{-5}$	1.159
Helium	679	0.278	4	5193	$3.50\ 10^{-5}$	0.0702

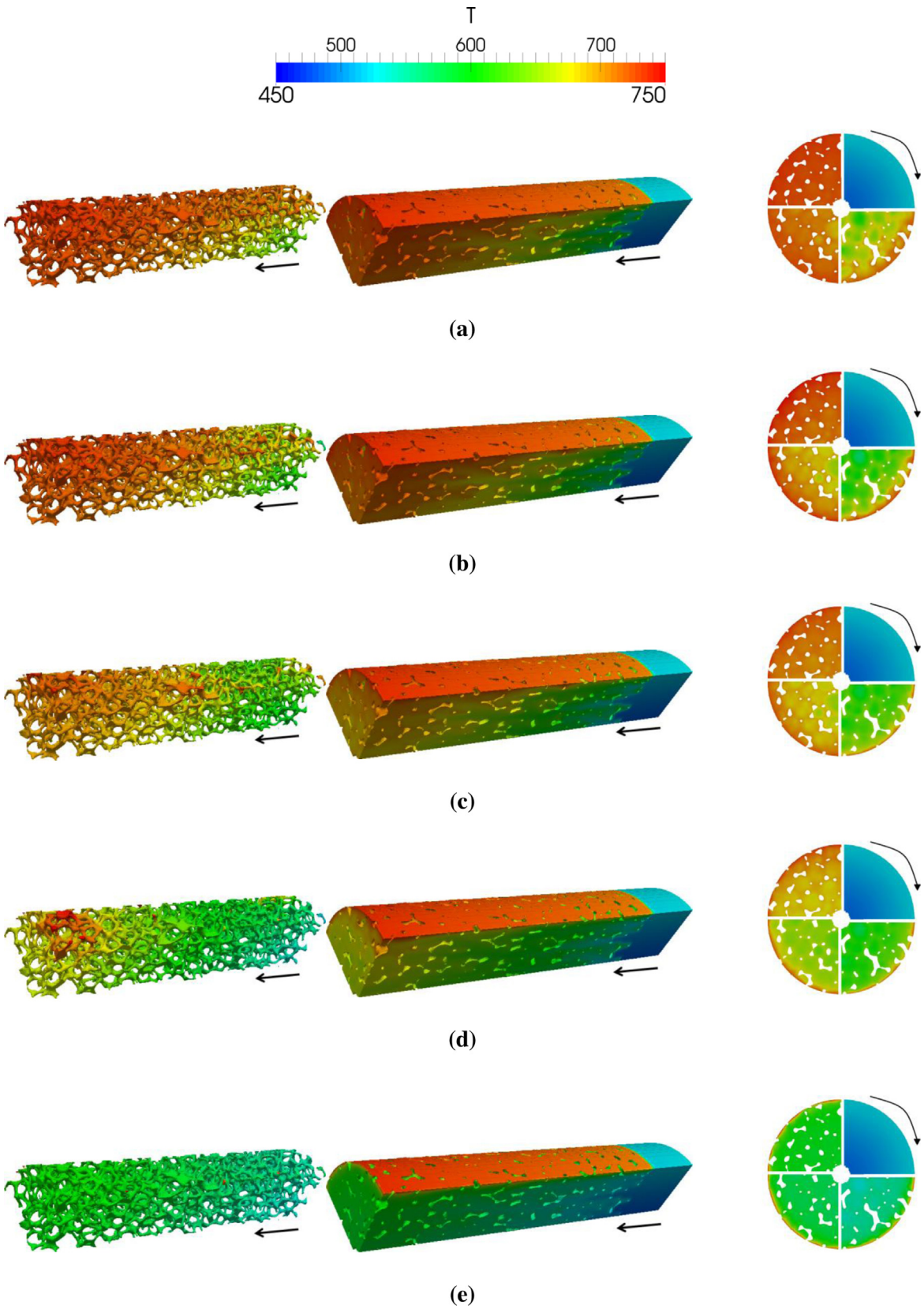

Fig. 4. Temperature distribution for different contact fraction between foam bed and reactor wall for the case of 30 Nl/min flow rate of nitrogen through an aluminum foam. From the left: foam bed (solid) temperature, gas phase temperature, and four slices equidistantly spaced along the axial coordinate (clockwise) illustrating the cross-sectional distribution of the gas phase temperature at four different axial positions. The arrow represents the inlet, flow direction, and the axial coordinate. The presented cases are 100% fraction of contact area (a), 20% (b), 10% (c), 5% (d), and 0% (e).

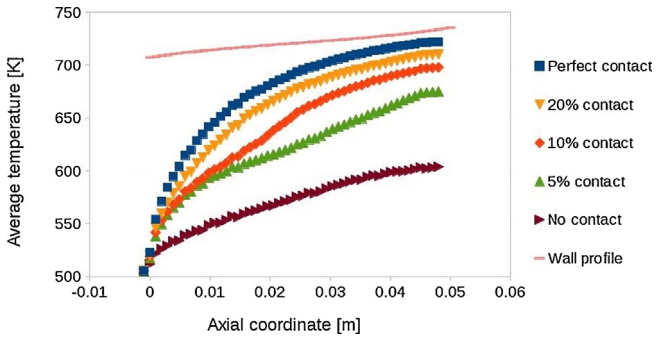

Fig. 5. Calculated axial profiles of average gas temperature for different fraction of contact between foam and tube wall.

used at the outlet, while at the inlet a combination of Dirichlet and Neumann boundary condition for pressure and velocity is set. The fluid velocity at the inlet is set to constant; this assumption seems justified by the flow distributor that was placed in front of the foam bed in the experimental configuration.

The gas inlet temperature is set to a radial distribution described by a 2nd order polynomial fitted from experimental data. The effective area averaged inlet temperature value is 505.5 K. The gas is heated up passing through the tube filled with the foam bed due to the heat coming from the solid wall, which represents the heat source. This leads to a higher gas temperature at the outlet compared to the inlet, depending on the quantity of heat transferred from the tube wall to the foam and to the gas by conductive and convective heat transport. The simulation runs were carried out in parallel mode on the "Lima" cluster at the High Performance Computing Center (Regionales RechenZentrum Erlangen, RRZE) of the Friedrich-Alexander-Universität Erlangen-Nürnberg, with 3×10^3 iterations and a residual error of 10^{-9}.

3.3. Methods of analysis

To examine the temperature distribution, one possibility is to extract the values for the gas phase averaged over an area. For this purpose, the gas phase temperature from the simulation results was "measured" on fifty slices (cross sections) that are equally spaced normal to the axial coordinate, starting from −1 mm up to 50 mm with the origin of the axial coordinate at the beginning of the foam bed (Fig. 3), and averaging the variable on the area of each slice. A single slice average was calculated because each of the slices has a different passage area due to the non-homogeneous porosity of the foam. Another method of visualization is a circle with four slices normal to the axial coordinate of the foam, equally spaced at the coordinate of −1 mm, 15.33 mm, 31.66 mm and 48 mm in the same coordinate system above (Fig. 4, right hand side). This configuration illustrates the cross-sectional temperature distribution in the gas phase and in clockwise direction its evolution along the flow path.

4. Results and discussion

4.1. Wall coupling

In the present case study the gas is heated up passing through the reactor tube filled with the foam. The tube wall shares 12% of its area with the foam. The starting point of the conjugated heat transfer analysis is the ideal case of perfect contact between the terminal struts of the foam and the wall, so the whole 12% area fraction can be used to conduct heat from the wall into the solid foam matrix. Progressively, some contact points were randomly selected and set to adiabatic in order to simulate the consequences of lack of contact in some parts of the foam. The variation was carried out from a percentage of 100% of shared area in contact down to 0%, i.e. no contact between foam and wall, thereby passing through intermediate fractions.

4.1.1. Effect of the contact fraction on the temperature profile

The results of the first investigation are shown in Fig. 4 for the cases of perfect contact, 20% of contact, 10%, 5%, and no contact between the foam and the tube wall for 30 Nl/min nitrogen flow rate in the Al foam. The results are also plotted in Fig. 5 as axial trends of the average gas temperature in the 50 slices sketched in Fig. 3. The average gas temperature features an increase of more than 200 K in the case of perfect contact. Even though less foam struts are connected to the reactor wall for the case of 20% contact area fraction, the average gas temperature at the outlet still shows an increase slightly lower but close to the one obtained for the perfect contact case. In the case of even less contact area, e.g. 5%, almost 200 K difference of inlet and outlet temperature are still observed. In fact, if the direct foam/tube wall contact is totally removed, the gas temperature rises only about 100 K from the inlet to the outlet, resulting in an outlet value of 600 K. A small region of warm gas near the wall can be seen in Fig. 4e, clearly indicating heating only from the tube wall and not by the foam.

This study proves that even a small connection between the foam and the tube wall is sufficient to contribute significantly to the heat up of the gas phase.

4.1.2. Effect of the randomization of the contact area

In order to check the sensitivity of the heat transfer behavior to the specific contact topology, the contact regions between foam and wall were selected with a randomizing algorithm, fixing the fraction of contact area and changing the local distribution of the selected contact points. An investigation of the influence of the position of the contact region for the cases of 10% and 5% of contact area was carried out. As shown in Fig. 6, for the 10% case the influence of the location of the contacting struts (randomly chosen for cases A, B and C) is weak, in fact less than 5 K difference for the gas temperature at the outlet for the three different distributions of contact points. For lower contact area, i.e. the 5% case, the influence of the randomly selected position of contacting struts for case A and B is slightly more important. Here, a different choice of the contact points results in more pronounced temperature differences, at least in some parts of the foam bed. Of course, such differences are still a minor effect when compared to the temperature increase obtained upon increasing the percentage of contact area which is the major influence.

4.1.3. Effect of the local distribution of the contact area

In industrial reactor applications the inlet zone is the region where the heat exchange requirements are more stringent. It is also usually the upper part of the reactor, so during the reactor loading process with the foam packing segments it is the last part that is filled. Accordingly, as a design rationale, special attention has to be paid with regard to the contact between the foam and the reactor wall at the top. This could, e.g., be realized by using foam packing segments which come very close to the tube diameter, avoiding the typical clearance that is otherwise necessary in order to avoid that the foam packing segments get stuck during the loading process. In order to analyze this in detail, the foam/wall contact was confined to the first third of the foam bed (Fig. 7a) and the contact efficiency was randomly decreased in order to analyze the influence of the wall coupling on the final gas temperature profile. As shown in Fig. 7b, the temperature profile shows a strong increase in the first part, and even with low contact area (e.g. 5% contact in the first third) the temperature at the outlet was approximately

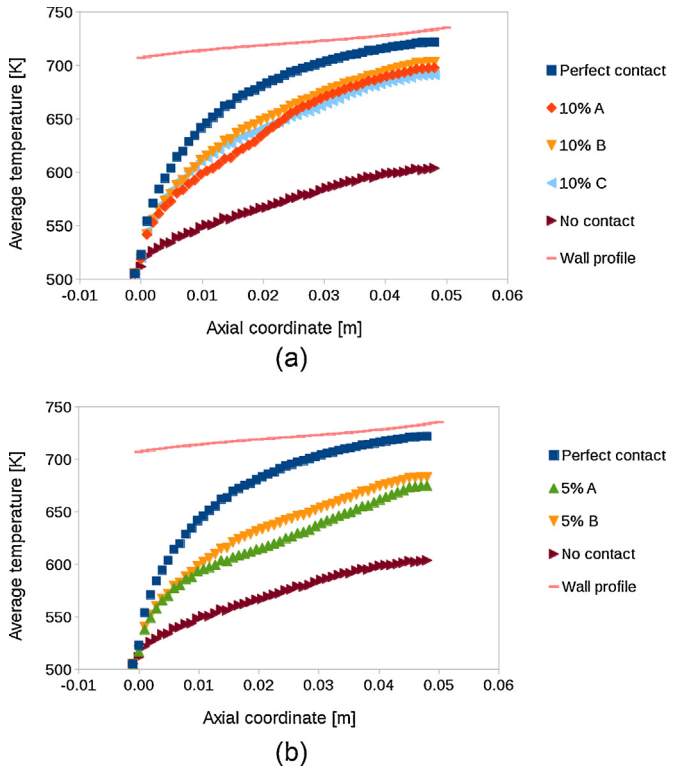

Fig. 6. Calculated axial profiles of average gas temperature for 30 Nl/min flow rate of nitrogen through an Al foam showing the effect of the randomization of the contact area for 10% (a) and 5% (b) contact fraction between foam and wall on the gas temperature profile along the axial coordinate.

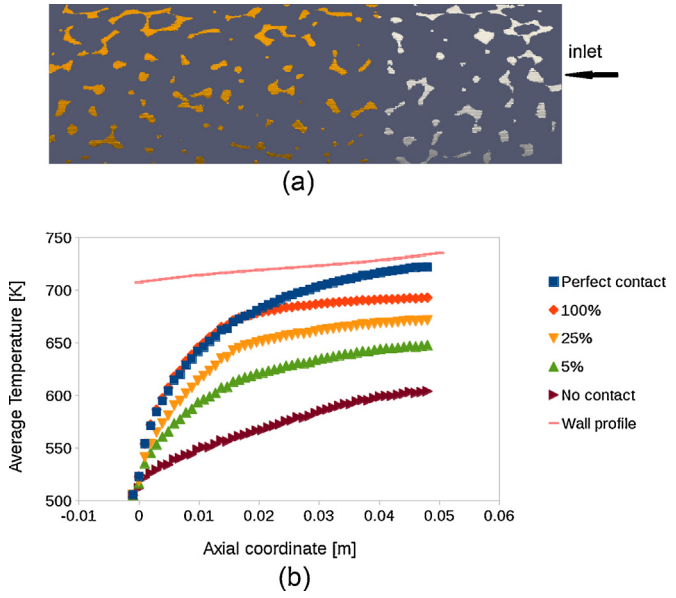

Fig. 7. Local distribution of the connected area in the case of contact in the first third of the reactor (i.e. at the inlet region), (a). Axial average gas temperature profiles for 30 Nl/min flow rate of nitrogen through an Al foam (b) starting with perfect contact between the foam bed and the reactor wall in the first third of the reactor, and then decreasing the area connected to the tube wall in the inlet region until the total absence of contact. The temperature values for perfect contact of the entire foam are shown for comparison.

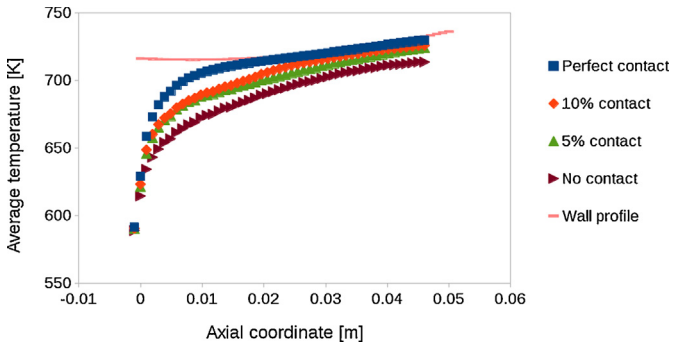

Fig. 8. Axial gas temperature profile for 30 Nl/min flow rate of helium through an Al foam starting with perfect contact between the foam bed and the reactor wall and decreasing the area connected to the tube wall to 10%, 5%, and to the total absence of contact.

50 K higher compared to the adiabatic case without any effective wall contact.

4.2. *Influence of the gas type*

Simulations and experiments with the foams were additionally carried out for 30 Nl/min flow rate of helium through an aluminum foam at the nominal gas inlet temperature of 500 K to investigate the influence of the gas type. For this, He was studied as a gas with significantly higher thermal conductivity (six times higher) compared to the previous case (values and reference temperatures are given in Table 1). The same simulation procedure as described above was carried out for this gas as well; starting from a perfect contact between the foam and the wall, the fraction of connected area was decreased until the complete absence of contact. In this case, the wall coupling had less influence on the gas temperature profile. In fact, helium requires less heat to increase its temperature compared to nitrogen (see Section 2.2). Besides, the higher conductivity of He enhances the heat transfer at the boundary between foam and wall via the indirect wall-gas-solid foam pathway, resulting in a lower impact of such boundary resistance on the overall heat transfer performance. The difference of the outlet gas temperatures between the perfect contact and the complete absence of contact case is about 20 K only (Fig. 8), while for nitrogen the difference is more than 100 K.

4.2.1. *Comparison with experiments*

Fig. 9 compares the axial gas phase temperature profiles calculated in the simulation with an average on 50 slices along the axial direction as illustrated in Fig. 3 and those measured in 10 points every 5 mm in the heat transfer experiments. Two setups are considered; a cylindrical foam only touching the tube wall in some points and another foam sintered to the tube wall (see Section 2.3). The foam in this latter case is directly connected to the wall (perfect contact), while in the first case the contact between the foam and the tube wall is loose.

The temperature profile at the tube wall, i.e. the heat source, exhibited small differences in these two experimental configurations. In order to minimize the impact of such differences on the comparison, a dimensionless temperature profile is used, defined as follows:

$$\vartheta(z) = \left(T_{i,gas}(z) - T^*_{gas}(z=0)\right) / \left(T(z=L)_{tube} - T^*_{gas}(z=0)\right)$$

where T_i is an area weighted average of the three measurements at different radii, while the difference between T_{tube} at the outlet and T^*_{gas} at the inlet represents the maximum possible temperature difference.

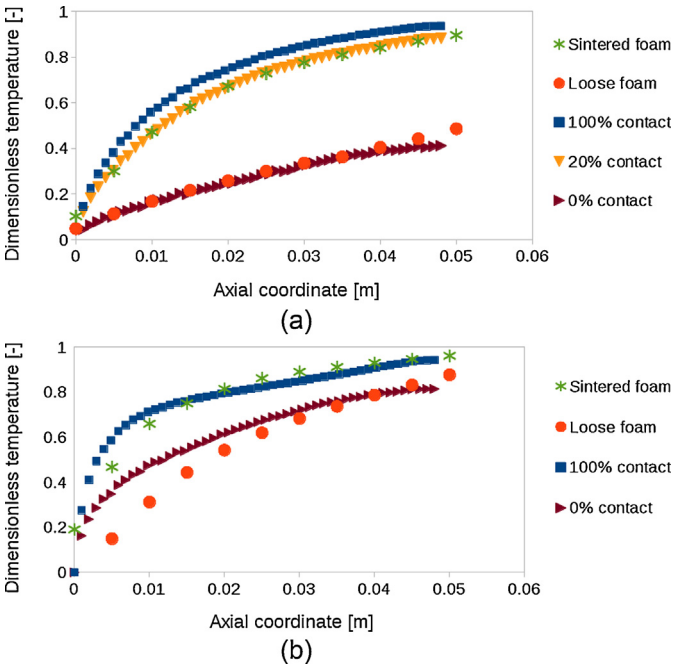

Fig. 9. Dimensionless axial gas temperature profile for 30 Nl/min flow rate of nitrogen (a) and helium flow (b) through an Al foam showing the comparison between simulation and experimental results. Two experimental profiles are presented: a foam sintered to the tube wall, and a foam loosely inserted into the same tube.

The data collected for the sintered foam follow the trend of the simulated cases for good foam/wall contact, and closely approach the 20% contact simulated temperature profiles. On the other hand, the data measured over the loose foam are close to the simulated case of no contact for both the investigated gases. The 20% contact profile is presented in Fig. 9 only for nitrogen, while it is omitted for helium due to the proximity with the 100% contact case. The differences between measured and simulated temperature profiles near the inlet for the helium case can partly be attributed to the usage of a constant thermal conductivity calculated for an average gas phase temperature. For the region near the inlet at relatively low temperatures, the real thermal conductivity will be lower than that calculated for the average temperature. This in turn results in an overestimation of the heat transfer in that region, predicting higher temperature values in the simulations. Additionally, the gas inlet conditions are more ideal in the simulation.

As main finding, the comparison between simulation and experiment confirms that wall coupling plays a key role in the heat transfer performance of open-cell foam structured reactors and that a strong improvement is obtained by securing a perfect contact between the tip of the foam struts and the tube wall, e.g. by diffusion bonding.

5. Conclusions

The aim of this work was to study numerically the conjugated heat transfer between a gaseous stream and metal foams inserted into a heated tube, in view of their use as structured catalyst supports in tubular reactors with heat exchange. The study is highly relevant for applications in the chemical process industry, where detailed knowledge is important in order to intensify the heat transfer in optimized reactors for strongly exo- or endothermic reactions.

For this purpose, several cases of a tube filled with metal foam supports were analyzed in detailed numerical studies, in analogy to heat transfer experiments carried out in a previous work [13]. In the heating runs, a foam geometry based on a 3D scan of a real metal foam sample made of aluminum alloy was investigated, considering a volumetric gas flow rate of 30 Nl/min. Two different gases, nitrogen and helium, were investigated in order to represent a process gas of low and of high thermal conductivity, respectively.

Initially, the case of perfect contact between foam and reactor wall was analyzed. Then, this case was manipulated in order to change the distribution and the percentage of contact area between the tube wall and the foam along the test tube. The study was repeated for a scenario wherein only the first third of the foam bed was in contact with the tube wall while the rest of the foam was regarded as thermally insulated at the wall. Finally, adiabatic conditions were set at the foam/wall interface in order to investigate the limiting case of complete absence of conduction between the foam and the reactor wall.

The results from this study show a strong dependence on the foam/wall coupling, which is a factor that decisively influences the temperature profiles. As a result of high practical relevance, it was demonstrated, and also validated with experimental heat transfer data, that already a quite low fraction of contact area (around 10. . .20%) is sufficient to significantly enhance the foam/wall heat transfer in the reactor, while a further increase of contact area will only result in a relatively small improvement.

Acknowledgements

The authors gratefully acknowledge the funding of the German Research Foundation (DFG), which, within the framework of its “Excellence Initiative”, supports the Cluster of Excellence “Engineering of Advanced Materials” at the Friedrich-Alexander-Universität Erlangen-Nürnberg (www.eam.fau.de).

The authors from Politecnico di Milano would like to thank Lorenzo Garancini for the experimental results obtained over the sintered foam. In addition, they gratefully acknowledge the financial support from the Italian Ministry of Education, University and Research, Rome (MIUR, Progetti di Ricerca Scientifica di Rilevante Interesse Nazionale, prot.2010XFT2BB), within the project IFOAMS: “Intensification of Catalytic Processes for Clean Energy, Low-Emission Transport and Sustainable Chemistry using Open-Cell Foams as Novel Advanced Structured Materials”.

References

[1] L.P. Lefebvre, J. Banhart, D.C. Dunand, Adv. Eng. Mater. 10 (2008) 775–787.
[2] V.C. Srivastava, K.L. Sahoo, Mater. Sci. –Poland 25 (2007) 733–753.
[3] A. Inayat, J. Schwerdtfeger, H. Freund, C. Körner, R.F. Singer, W. Schwieger, Chem. Eng. Sci. 66 (2011) 2758–2763.
[4] M. Klumpp, A. Inayat, J. Schwerdtfeger, C. Körner, R.F. Singer, H. Freund, W. Schwieger, Chem. Eng. J. 242 (2014) 364–378.
[5] A. Inayat, M. Klumpp, M. Lämmermann, H. Freund, W. Schwieger, Chem. Eng. J. 287 (2016) 704–719.
[6] A. Inayat, H. Freund, A. Schwab, T. Zeiser, W. Schwieger, Adv. Eng. Mater. 13 (2011) 990–995.
[7] A. Inayat, H. Freund, T. Zeiser, W. Schwieger, Chem. Eng. Sci. 66 (2011) 1179–1188.
[8] B. Dietrich, G. Schell, E.C. Bucharsky, R. Oberacker, M.J. Hoffmann, W. Schabel, M. Kind, H. Martin, Int. J. Heat Mass Tran. 53 (2010) 198–205.
[9] J. Banhart, Prog. Mater. Sci. 46 (2001) 559–632.
[10] J. Banhart, MRS Bull. 28 (2003) 290–295.
[11] J. Banhart, Int. J. Veh. Des. 37 (2005) 114–125.
[12] J. Banhart, D. Weaire, Phys. Today 55 (2002) 37–42.
[13] E. Bianchi, T. Heidig, C.G. Visconti, G. Groppi, H. Freund, E. Tronconi, Chem. Eng. J. 198–199 (2012) 512–528.
[14] M.V. Twigg, J.T. Richardson, Ind. Eng. Chem. Res. 46 (2007) 4166–4177.
[15] D. Edouard, M. Lacroix, C.P. Huu, F. Luck, Chem. Eng. J. 144 (2) (2008) 299–311.
[16] T. Zeiser, M. Steven, H. Freund, P. Lammers, G. Benner, F. Durst, J. Bernsdorf, Philos. Trans. R. London, Ser. Soc. A 360 (2002) 507–520.
[17] E. Bianchi, W. Schwieger, H. Freund, Adv. Eng. Mater. (2015), http://dx.doi.org/10.1002/adem.201500356.
[18] O. Smorygo, V. Mikutski, A. Marukovich, Y. Vialiuha, A. Ilyushchanka, N. Mezentseva, G. Alikina, Z. Vostrikov, Y. Fedorova, V. Pelipenko, R. Bunina, V. Sadykov, Int. J. Hydrogen Energy 34 (2009) 9505–9514.

[19] A. Sirijaruphan, J.G. Goodwin Jr., R.W. Rice, D. Wei, K.R. Butcher, G.W. Roberts, J.J. Spivey, Appl. Catal. A 281 (2005) 1–9.
[20] P. Mülheims, B. Kraushaar-Czarnetzki, Ind. Eng. Chem. Res. 50 (2011) 9925–9935.
[21] I. Gräf, A.K. Rühl, B. Kraushaar-Czarnetzki, Chem. Eng. J. 244 (2014) 234–242.
[22] A. Montebelli, C.G. Visconti, G. Groppi, E. Tronconi, C. Ferreira, S. Kohler, Catal. Today 215 (2013) 176–185.
[23] H.N.G. Wadley, Adv. Eng. Mater. 4 (2002) 726–733.
[24] E. Bianchi, T. Heidig, C.G. Visconti, G. Groppi, H. Freund, E. Tronconi, Catal. Today 216 (2013) 121–134.
[25] E. Bianchi, G. Groppi, W. Schwieger, E. Tronconi, H. Freund, Chem. Eng. J. 264 (2015) 268–279.
[26] J.R. Davis, Aluminum and Aluminum Alloys, vol. I, M.P.A., International, New York, 1993, pp. p. 784 (ASM International: Handbook Committee ed).
[27] L. Giani, G. Groppi, E. Tronconi, Ind. Eng. Chem. Res. 44 (2005) 4993–5002.
[28] C.Y. Zhao, T.J. Lu, H.P. Hodson, Int. J. Heat Mass Transfer 47 (2004) 2927–2939.
[29] G. Incera Garrido, B. Kraushaar-Czarnetzki, Chem. Eng. Sci 65 (2010) 2255–2257.
[30] OpenFOAM, http://www.openfoam.org, retrieved in November 2015.
[31] K.K. Bodla, J.Y. Murthy, S.V. Garimella, XMT-based direct simulation of flow and heat transfer through open-cell aluminum foams, in: in: Thermal and Thermomechanical Phenomena in Electronic Systems (ITherm), 12th IEEE Intersociety Conference, 2010, pp. 1–9.
[32] J. Grosse, B. Dietrich, G. Incera Garrido, P. Habisreuther, N. Zarzalis, H. Martin, M. Kind, B. Kraushaar-Czarnetzki, Ind. Eng. Chem. Res. 48 (2009) 10395–10401.